DOI: 10.1002/chem.200600097

# One-Electron Oxidation Pathways during β-Cyclodextrin-Modified $TiO_2$ Photocatalytic Reactions

**Takashi Tachikawa, Sachiko Tojo, Mamoru Fujitsuka, and Tetsuro Majima*[a]**

**Abstract:** The photocatalytic one-electron oxidation reactions of aromatic sulfides using the carboxymethyl-β-cyclodextrin (CM-β-CD)-modified $TiO_2$ nanoparticles ($TiO_2$/CM-β-CD) were investigated by using nano- and femtosecond transient absorption spectroscopies. The one-electron oxidation processes of the substrate (S) by the valence band hole ($h_{VB}^+$) at the $TiO_2$ surface and the trapped hole at the adsorption site of the CM-β-CD ($h_{CD}^+$) were examined. The transient absorption spectra and time traces observed for the charge carriers and the radical cation of S ($S^{\bullet+}$) revealed that the one-electron oxidation reaction of S during the nano- and femtosecond laser flash photolyses of $TiO_2$/CM-β-CD is significantly enhanced relative to bare $TiO_2$. The kinetics of the decay and the dimerization processes between $S^{\bullet+}$s are discussed on the basis of the results obtained by the pulse radiolysis technique.

**Keywords:** cyclodextrins · electron transfer · laser-flash photolysis · radical ions · titanium dioxide

## Introduction

Nanostructured composite materials, either as such or as surface-supported architectures, are now the focus of intense fundamental and applied research in a number of areas.[1] Particularly, areas of research that aim to develop the basic science needed for integrating organic and inorganic compounds into semiconductor nanoparticles are driving what seems to be the advent of an entirely new set of nanoscale functional architectures with limitless applications.

Cyclodextrins (CDs) are versatile host molecules that can include a variety of organic and inorganic compounds. Therefore, they have been employed as biomimetic cavities for analytical applications and for industrial applications, such as solubilization agents and drug carriers.[2] Recently, CDs have been modified as electron-donating and molecular-recognizing agents on semiconductor nanoparticles.[3–8] In general, the chemisorption of CDs onto semiconductors increases the stability of particles against aggregation and enhances the yield of photo-induced charge-transfer reactions.[5] Thus, the modification of CDs on the $TiO_2$ photocatalyst shows a significant enhancement effect on degradation processes of a pollutant.[3,4] By using low-temperature EPR and cyclic voltammetry, Dimitrijevic and co-workers observed that the valence-band holes ($h_{VB}^+$) localize at the carboxy groups of surface-conjugated carboxyethyl-β-CD.[6] More recently, it has been reported that CDs appear to act as bifunctional linkers when interacting with anatase $TiO_2$ nanorods under UV light, resulting in super-long $TiO_2$-containing wires.[7]

Although a great deal of research has been conducted on the effects of surface-bound CDs on the charge separation and photodecomposition of organic compounds during $TiO_2$ photocatalytic reactions, to our knowledge, no quantitative studies have been reported for the one-electron oxidation processes of organic compounds included in the CD nanocavity adsorbed on $TiO_2$ using time-resolved spectroscopy. Much less information is also available on the kinetics of association and dissociation of radical ions, which are generated from $TiO_2$ photocatalytic reactions, with CDs. Such information is very useful for the controlled release of guest molecules, such as drugs, from the semiconductor-based, host-guest hybrid nanoparticles by the photo-induced electron-transfer reaction.

We have studied the photocatalytic one-electron oxidation reactions of aromatic compounds using carboxymethyl (CM)-β-CD-modified $TiO_2$ nanoparticles ($TiO_2$/CM-β-CD) based on nano- and femtosecond transient absorption measurements. Aromatic sulfides were chosen as the substrate (S) because of 1) a number of studies on CD complexation

[a] Dr. T. Tachikawa, S. Tojo, Prof. Dr. M. Fujitsuka, Prof. Dr. T. Majima
The Institute of Scientific and Industrial Research (SANKEN)
Osaka University
Mihogaoka 8–1, Ibaraki, Osaka 567–0047 (Japan)
Fax: (+81) 6-6879-8496
E-mail: majima@sanken.osaka-u.ac.jp

Supporting information for this article is available on the WWW under http://www.chemeurj.org/ or from the author.

  

with benzene derivatives;[9,10] 2) their importance as intermediates in many chemical processes including those of organic synthesis,[11] and environmental,[12] and biological significance;[13,14] and 3) the specific spectroscopic properties of S and the radical cations ($S^{\bullet+}$), which have negligible absorption at 355 and 330 nm as the excitation wavelength for $TiO_2$ and absorption in the visible region (abound 400–600 nm), respectively.[15–19] In addition, our preliminary work revealed that $S^{\bullet+}$, which is generated from the one-electron oxidation processes during the pulse radiolysis of an aqueous solution, is excluded from the β-CD nanocavity in the nano- to microsecond time domain.[20]

The overall goal of the present research is to clarify the influences of CDs on the one-electron oxidation reactions of S during $TiO_2$ photocatalytic reactions and the subsequent reactions of the resultant $S^{\bullet+}$. In addition, the present findings not only verify the applicability of the $TiO_2$/CM-β-CD nanocomposite material, but also provide important information about the mechanisms of the $TiO_2$ photocatalytic oxidation reactions in the subpico- to microsecond time range.

## Results and Discussion

**Structure of the $TiO_2$/CM-β-CD/substrate hybrid nanoparticles**: The CM-β-CD has an average of 3.5 carboxymethyl groups per CD.[21] The procedure commonly used to prepare CM-β-CD leads to predominant substitution of the carboxymethyl groups at the secondary hydroxyl sites, but with some substitution at the primary hydroxyl groups as well. From the $^1H$ NMR measurements, the number of β-CD and CM-β-CD bound to each $TiO_2$ nanoparticle in acidic water (pH 2) was estimated to be zero or one and five or six for β-CD and CM-β-CD, respectively, suggesting that CM-β-CD is adsorbed on the surface of $TiO_2$ particles through the chelating complex of the carboxyl groups with surface Ti ions.[22] Dimitrijevic et al. reported that, based on IR spectroscopy, oxygen atoms from the carboxy groups of carboxyethyl-β-CD are bound to the surface Ti atoms of $TiO_2$ particles.[6] The attachment of carboxy groups onto β-CD can facilitate oxidation by providing a deeper trapping site that attracts holes in primary events as discussed below. Hence, in the case of β-CD, no enhancement effect on the one-electron oxidation process of the substrate (S) was observed under the present conditions (see Figure S1 in the Supporting Information).

As shown in Figure 1, a visible absorption band very similar to those observed for electron-donating bidentate ligands such as catechol and $TiO_2$ nanoparticles appeared when 4-(methylthio)phenol (MTP) was added to the CM-β-CD-modified $TiO_2$ colloidal aqueous solution ($TiO_2$/CM-β-CD), indicating the formation of the charge transfer (CT) complex between MTP and $TiO_2$.[19d,e,23–26] On the other hand, no CT bands were observed for the other substrates S.

To date, two types of interactions with $TiO_2$ have been reported: coordinative covalent bonding (CCB) between the adsorbates and the $Ti^{IV}$ ions on the $TiO_2$ surface, and physical adsorption (PA) between arenes and $TiO_2$. The CCB-type interactions give rise to ligand-to-metal charge-transfer (LMCT) interactions between the adsorbates and $Ti^{IV}$ ions owing to the low-lying empty $t_{2g}$ orbitals of the $Ti^{IV}$ centers in octahedral environments.[24] Indeed, the electron-rich aromatic compounds with functional groups, such as hydroxy and carboxy groups, display LMCT bands in the visible region. Therefore, from the structure of the inclusion complex between MTP and CM-β-CD,[20] one can predict that the CT complexes prefer the CCB-type rather than the PA-type interaction in the present systems, as shown in Figure 2.

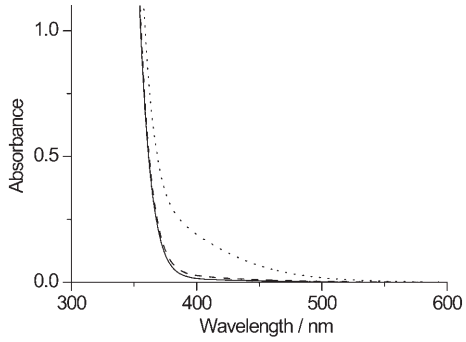


Figure 1. Steady-state UV/Vis absorption spectra observed for the bare $TiO_2$ (——) colloidal solution, and the $TiO_2$ colloidal solutions containing MTP (0.5 mM) in the absence (-----) and presence (•••••) of CM-β-CD at room temperature.

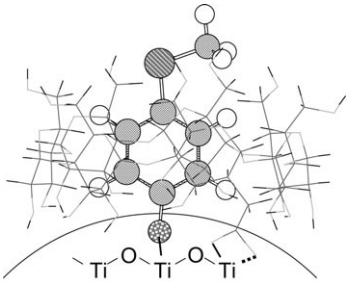


Figure 2. Model of the inclusion of MTP in the CM-β-CD adsorbed on the $TiO_2$ nanoparticle. Only one $-CH_2COOH$ group of CM-β-CD is depicted here.

The fact that no CT bands were observed for the other S is mainly attributable to the poor electron-donating properties of S relative to MTP, which has the lowest ionization potential (IP) (Table 1), because both binding constants of S with $TiO_2$ ($K_{ad}$) and with CM-β-CD ($K_{CD}$) decreased in the order of 4-(methylthio)phenylacetic acid (MTPA) ≫ MTP ≫ 4-(methylthio)phenyl methanol (MTPM) > 4-(methylthio)toluene (MTT), as listed in Tables 1 and 2, respectively.

**Hole trapping by CM-β-CD on $TiO_2$**: First, in order to confirm the hole trapping process by CM-β-CD adsorbed on the $TiO_2$ surface, we observed the nanosecond transient absorption spectra during the 355 nm laser photolysis of an Ar-saturated $TiO_2$ colloidal aqueous solution in the absence and presence of CM-β-CD (Figure 3). As mentioned in the

  

Table 1. Oxidation potentials ($E_{ox}$) of substrates (S) and the molar absorbance coefficients of $S^{\bullet+}$ ($\varepsilon^{\bullet+}$).

| S | X[a] | $E_{ox}$ [V vs. NHE] | IP [eV][b] | $K_{ad}$ [$M^{-1}$][c] | $\varepsilon^{\bullet+}$ [$M^{-1}cm^{-1}$] ($\lambda$ [nm])[d] |
|---|---|---|---|---|---|
| MTP | OH | 1.42 | 7.15 | 2400 | 4000 (530) |
| MTT | $CH_3$ | 1.57 | 7.26 | 20 | 6700 (545) |
| MTPM | $CH_2OH$ | 1.59 | 7.28 | 180 | 5500 (545) |
| MTPA | $CH_2COOH$ | 1.67 | 7.34 | 12000 | 5000 (550) |

[a] $X-C_6H_4-SCH_3$. [b] The molecular geometries were optimized firstly by the semiempirical quantum chemical method AM1. Finally, B3LYP/6–31G(d) was used for the full geometry optimization in the gas phase. The zero-point vibrational energies and the vibrational contribution to the enthalpy calculated at the B3LYP/6–31G(d,p) level were scaled by a factor of 0.9806.[27] The quantum chemical calculations were accomplished by Gaussian 98.[28] [c] Determined from UV/Vis absorption measurements at pH 2.[19e] [d] Reference [20].

Table 2. Molar absorbance coefficients ($\varepsilon$) for free S ($\varepsilon_0$) and S/CD ($\varepsilon_{CD}$), and binding constant ($K_{CD}$) for the S/CD complexes.

| S[a] | CD | $\varepsilon_0$[b] [$M^{-1}cm^{-1}$] | $\varepsilon_{CD}$[b] [$M^{-1}cm^{-1}$] | $K_{CD}$[b] [$M^{-1}$] |
|---|---|---|---|---|
| MTP | CM-β-CD | 9400 | 7400 | $250\pm20$ |
| MTT | β-CD | 9100 | 7000 | $150\pm20$ |
| | CM-β-CD | 9100 | 7100 | $140\pm20$ |
| MTPM | CM-β-CD | 11600 | 9100 | $150\pm20$ |
| MTPA | CM-β-CD | 12000 | 10500 | $300\pm30$ |

[a] [S] = 0.05 mM. [b] Determined from UV/Vis absorption measurements.[20] The $\varepsilon$ values were determined at the maximum wavelength.

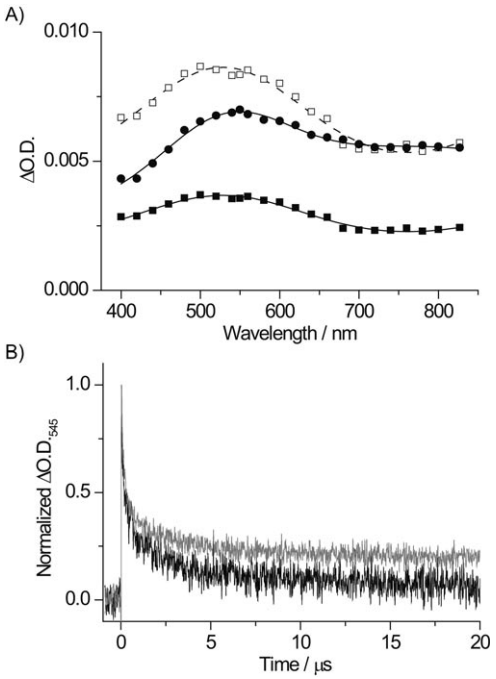


Figure 3. A) Nanosecond transient absorption spectra observed at 0.1 μs after the laser flash during the 355 nm laser photolysis of the Ar-saturated $TiO_2$ colloidal aqueous solution in the absence (■) and presence (●) of CM-β-CD (0.5 mM). The normalized transient absorption spectrum observed during the 355-nm laser photolysis of the Ar-saturated $TiO_2$ colloidal aqueous solution in the absence of CM-β-CD (□). B) Time profiles of ΔO.D. at 545 nm observed for $TiO_2$ (black) and $TiO_2$/CM-β-CD (gray).

introduction, the valence band hole ($h_{VB}^+$) and the conduction band electron ($e_{CB}^-$) are generated in the $TiO_2$ particles during the band gap excitation [Eq. (1)].

$$TiO_2 + h\nu \rightarrow h_{VB}^+ + e_{CB}^- \quad (1)$$

The fast charge recombination and transfer kinetics of these photogenerated carriers have been studied in detail by several groups.[29–36] Although most charge carriers quickly recombine, a minority are trapped at the surface of the particles as given by Equation (2), in which $h_{tr}^+$ and $e_{tr}^-$ denote the trapped holes and electrons, respectively.

$$h_{VB}^+ \rightarrow h_{tr}^+,\ e_{CB}^- \rightarrow e_{tr}^- \quad (2)$$

Recent transient absorption studies have revealed that the absorption spectra of these charge carriers overlap in the visible wavelength range. According to previous studies,[35,36] the transient absorption spectrum observed for bare $TiO_2$ is explained well by the absorption bands of $h_{tr}^+$ and $e_{tr}^-$.[37]

On the other hand, in the presence of CM-β-CD, a significant difference in the spectral shape was observed. For comparison, the normalized transient absorption spectrum observed for bare $TiO_2$ is also shown in Figure 3A. The decrease in ΔO.D. around 400–650 nm clearly indicates that the scavenging of holes by CM-β-CD has occurred. The increase in the lifetime of $e_{tr}^-$ by the modification of CM-β-CD also supports the fact that the photogenerated holes, which can recombine with $e_{tr}^-$, are trapped by CM-β-CD adsorbed on the $TiO_2$ surface. Using the $\varepsilon$ value of 420 $M^{-1}cm^{-1}$ at 520 nm for $h_{tr}^+$,[38] one can estimate the decrease of $(4.1\pm1.0)\times10^{-6}$ M in the concentration of $h_{tr}^+$ owing to the hole transfer from the photogenerated holes to CM-β-CD adsorbed on the $TiO_2$ surface. The yield of the hole scavenging by CM-β-CD was also estimated to be about 10% using the absorbed photon concentration of $4.4\times10^{-5}$ M.

**One-electron oxidation reaction of S**: As already mentioned, S with functional groups such as hydroxy or carboxy groups inside CM-β-CD can be directly attached to the surface of $TiO_2$. Therefore, to exclude the effect of direct adsorption of S onto the $TiO_2$ surface, we examined the one-electron oxidation process of MTT, which has no adsorption group, during the 355-nm laser-flash photolysis of $TiO_2$ and $TiO_2$/CM-β-CD.

Figure 4A shows the transient spectra observed for $TiO_2$/CM-β-CD in the presence of MTT (0.5 mM) ($TiO_2$/CM-β-CD/MTT). A broad transient absorption band with a peak around 550 nm was observed immediately after the laser flash and was assigned to $MTT^{\bullet+}$.[15,20] The increase in ΔO.D. within the laser duration of 5 ns clearly indicates that the one-electron oxidation process of MTT was enhanced as a result of the modification of CM-β-CD (Figure 4B, traces c and d). For the bare $TiO_2$, a transient signal due to $MTT^{\bullet+}$ was observed at $>0.5$ μs after the laser flash (Figure 4B, traces a and b), suggesting that MTT is oxidized by the indi-

  

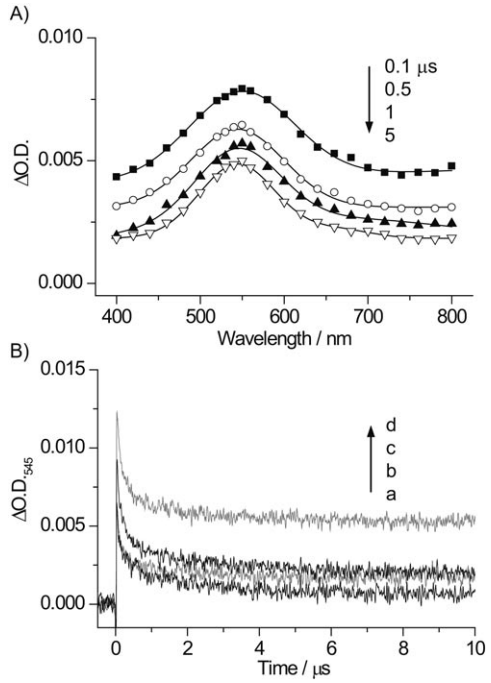


Figure 4. A) Nanosecond transient absorption spectra observed after the laser flash during the 355-nm laser photolysis of the Ar-saturated $TiO_2$ colloidal aqueous solution in the presence of CM-β-CD (0.5 mM) and MTT (0.5 mM). B) Time profiles of ΔO.D. at 545 nm observed for $TiO_2$ (a), $TiO_2$/MTT (b), $TiO_2$/CM-β-CD (c), and $TiO_2$/CM-β-CD (d) systems.

rect one-electron oxidation process of the free S ($S_f$) with $h_{tr}^+$ as given by Equation (3).[39,40]

$$h_{tr}^+ + S_f \rightarrow S_f^{\cdot+} \quad (3)$$

As previously reported,[41] the energy of $h_{tr}^+$ is in the range of $+1.6\,V \leq \equiv TiO^{\bullet-}, H^+/\equiv TiOH \leq +1.7\,V$ versus NHE, which is sufficient for the one-electron oxidation of S, as summarized in Table 1.

From these experimental results, we describe the CM-β-CD-mediated one-electron oxidation processes of S included in CM-β-CD ($S_{CD}$) adsorbed on the $TiO_2$ surface as follows in Equations (4) and (5), in which $h_{CD}^+$ ($CM^{\cdot+}$-β-CD) is the hole trapped at the carboxy groups of CM-β-CD adsorbed on the $TiO_2$ surface.[6]

$$h_{VB}^+ \rightarrow h_{CD}^+(CM^{\cdot+}\text{-}\beta\text{-CD}) \quad (4)$$

$$h_{CD}^+(CM^{\cdot+}\text{-}\beta\text{-CD}) + S_{CD} \rightarrow S_{CD}^{\cdot+} \quad (5)$$

The enhancement effect similar to that of MTT from the modification of CM-β-CD was observed for all S, as summarized in Table 3. However, in the cases of MTP, MTPM, and MTPA, which have an adsorption group, the direct one-electron oxidation process of the surface-bound S ($S_a$) by $h_{VB}^+$ within the laser pulse duration of 5 ns should be included in the reaction scheme as given by Equation (6).

$$h_{VB}^+ + S_a \rightarrow S_a^{\cdot+} \quad (6)$$

Table 3. Concentrations of $S^{\cdot+}$ observed for the $TiO_2$/S and $TiO_2$/CM-β-CD/S systems.

| S | $[S^{\cdot+}]^{[a]}$ [μM] | | $[S^{\cdot+}]^{[b]}$ [μM] | |
|---|---|---|---|---|
| | $TiO_2$ | $TiO_2$/CM-β-CD | $TiO_2$ | $TiO_2$/CM-β-CD |
| MTP | 1.1 | 2.8 (+1.7)[c] | 1.1 | 1.0 (−0.1)[c] |
| MTT | ~0 | 0.4 (+0.4)[c] | 0.2 | 0.5 (+0.3)[c] |
| MTPM | ~0 | 1.1 (+1.1)[c] | 0.4 | 0.4 (±0.0)[c] |
| MTPA | 1.2 | 3.4 (+2.2)[c] | 0.4 | 0.4 (±0.0)[c] |

[a] Obtained immediately after the laser flash. Error within ±15%. [b] Obtained at 20 μs after the laser flash. Error within ±10%. [c] Calculated by subtracting the $[S^{\cdot+}]$ value in the absence of CM-β-CD from that in the presence of CM-β-CD.

As summarized in Table 3, the effect of the adsorption of S on the direct one-electron oxidation process [Eq. (6)] with $h_{VB}^+$ is clearly confirmed by a comparison between increases in the initial concentration of $S^{\cdot+}$ determined for MTT (+0.4 μM) and MTPM (+1.1 μM), which have similar $E_{ox}$ and $K_{CD}$ values. Note that almost the same increase in the $[S^{\cdot+}]$ values at delay times of about 0 and 20 μs was obtained for MTT, suggesting that $MTT^{\cdot+}$ is excluded from the β-CD nanocavity into the bulk solution because of the hydrophobic nature of the cavity ($K_{CD} < 10\,M^{-1}$ for $MTT^{\cdot+}$).[20]

Interestingly, it was also found that the absorption peak of $MTP^{\cdot+}$ changed by approximately 15–20 nm in the several microsecond time domain after the laser irradiation (Figure 5). The observed red shift relative to that obtained in acidic water (pH 2) was also confirmed from the femto-

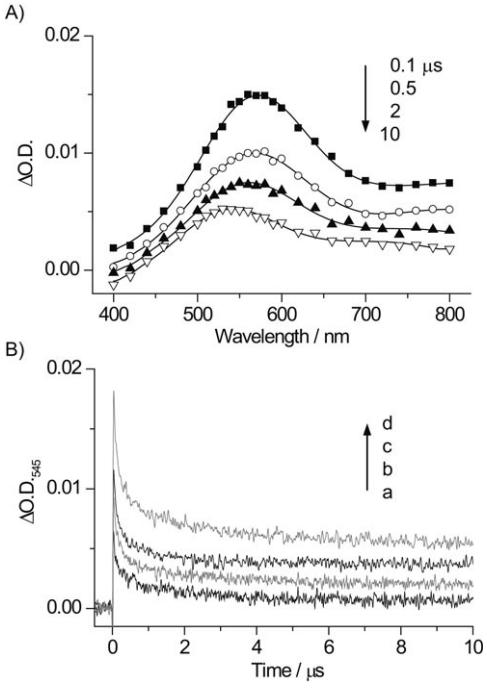


Figure 5. A) Transient absorption spectra observed after the laser flash during the 355-nm laser photolysis of the Ar-saturated $TiO_2$ colloidal aqueous solution in the presence of CM-β-CD (0.5 mM) and MTP (0.5 mM). B) Time profiles of ΔO.D. at 545 nm observed for $TiO_2$ (a), $TiO_2$/MTP (b), $TiO_2$/CM-β-CD (c), and $TiO_2$/CM-β-CD/MTP (d) systems.

  

second transient absorption measurements (see Figure 7D and Figure S2 in the Supporting Information).

A similar red shift was also observed for MTPM and MTPA in both the absence and presence of CM-β-CD, while no peak shift was observed for MTT as shown in Figure 4A. Similar changes in the absorption and emission characteristics of several compounds have been observed when they are adsorbed on colloidal semiconductors.[42,43] Therefore, the electronic interaction between $S^{\bullet+}$ and $TiO_2$ and the surface polarity altered the energetics of the ground and excited states of $S^{\bullet+}$.

As shown in Figure 6A, the time traces for the peak shift ($\Delta\nu$) from the absorption maximum observed at 20 μs after

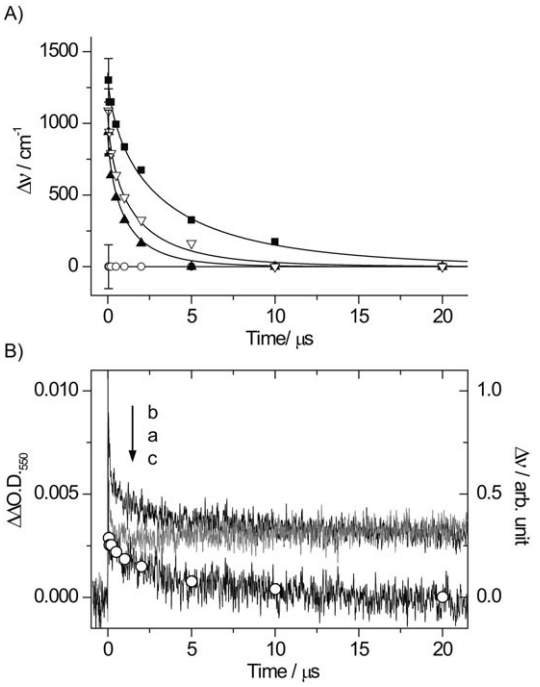


Figure 6. A) Time dependence of the peak shift ($\Delta\nu$) from the transient absorption spectra observed at 20 μs after the laser flash during the 355-nm laser photolysis of the Ar-saturated $TiO_2$/CM-β-CD colloidal aqueous solution in the presence of MTP (■), MTT (○), MTPM (▲), and MTPA (▽) (0.5 mM). Solid lines indicate the results fitted by the stretched exponential function. B) The differential time traces obtained for $TiO_2$ (a) and $TiO_2$/CM-β-CD (b) by subtracting the time trace observed in the absence of MTP from that in the presence of MTP. The black line (c) indicates the differential time trace obtained by subtracting line a from line b. The relative $\Delta\nu$ values for MTP are shown for comparison (○).

the laser flash were well reproduced using a stretched exponential function as given by Equation (7), in which $\tau_s$ is the apparent average lifetime of the surface-bound $S^{\bullet+}$ and $\alpha$ is a heterogeneous parameter.[44,45]

$$\Delta\nu(t) = \Delta\nu_{max}(t)\exp(1-(t/\tau_s)^{\alpha}) \quad (7)$$

For example, the $\tau_s$ and $\alpha$ values were determined to be 1.5 μs and 0.65, respectively, for MTPA (Table 4). The lack of a relationship between $\tau_s$ and $K_{ad}$ suggests that $S^{\bullet+}$ adsor-

Table 4. Fitting parameters for the time-dependent peak shift.

| S | $\Delta\nu_{max}$ [$cm^{-1}$] | $\tau_s$ [μs] | α |
|---|---|---|---|
| MTP | 1300±150 | 3.0±0.5 | 0.65±0.05 |
| MTPM | 1050±150 | 1.2±0.3 | 0.70±0.05 |
| MTPA | 1180±150 | 1.5±0.3 | 0.65±0.05 |

bed on the $TiO_2$ surface cannot be desorbed from the surface on a microsecond time scale. It seems that the $\tau_s$ values determined are close to those ($\tau_s$ = (3.8±0.5) μs) determined for $S^{\bullet+}$ adsorbed on $TiO_2$ nanoparticles in acetonitrile.[19e] In addition, it was found that a good relationship exists between the time evolutions of the signal intensity and peak shift of $S^{\bullet+}$ as demonstrated in Figure 6B. Therefore, we assumed that the observed peak shift after the laser flash is attributable to the heterogeneous charge recombination kinetics with $e_{tr}^-$ and the formation of $S_f^{\bullet+}$ by the indirect one-electron oxidation process [Eq. (3)]. Similar [$S^{\bullet+}$] values obtained at 20 μs for $TiO_2$ and $TiO_2$/CM-β-CD in the presence of MTP, MTPM, and MTPA also support our conclusion (Table 3).

**Interfacial hole-transfer dynamics**: In this section, we examine the interfacial hole-transfer dynamics from the photogenerated holes to MTP adsorbed on the $TiO_2$ surface by femtosecond transient-absorption measurements.

Figure 7 shows the time evolution of the transient-absorption spectra observed during the 330 nm laser photolysis (5 μJ $pulse^{-1}$, 200 fs FWHM) of the $TiO_2$ (A), $TiO_2$/CM-β-CD (B), and $TiO_2$/CM-β-CD/MTP (C) solutions. For $TiO_2$ and $TiO_2$/CM-β-CD (in the absence of S), a broad absorption band in the wavelength range from 500 to 700 nm was observed. On the other hand, an absorption band with a peak around 575 nm was clearly observed for $TiO_2$/CM-β-CD/MTP (Figure 7D). This absorption band is practically identical to that assigned to $MTP^{\bullet+}$ obtained in the nanosecond time domain (Figure 5A). A similar transient absorption spectrum with a peak around 575 nm was also confirmed by the 400 nm laser photolysis (10 μJ $pulse^{-1}$, 200 fs FWHM) of $TiO_2$/CM-β-CD/MTP, that is, the direct excitation of the CT complex between MTP and $TiO_2$ (see Figure S2 in the Supporting Information). In the case of the bare $TiO_2$, no clear absorption band from $MTP^{\bullet+}$ was observed because of the low concentration of the surface-bound MTP on $TiO_2$.

As shown in Figure 7E, a double exponential decay process with time constants of (4.0±0.5) (38%) and (15±5) ps (62%) were determined for $TiO_2$/CM-β-CD/MTP (●) at 700 nm, which is assigned to the shallowly trapped hole as discussed below, while a time constant of (18±5) ps was determined for $TiO_2$/CM-β-CD (△).

In general, the carriers generated in semiconductor nanoparticles are in a nonequilibrium distribution immediately after excitation. The hot carriers, such as free electrons and holes having a finite kinetic energy, relax within the conduction and valence bands, respectively, and then are trapped at various defect sites, that is, the shallow and deep trapping

  

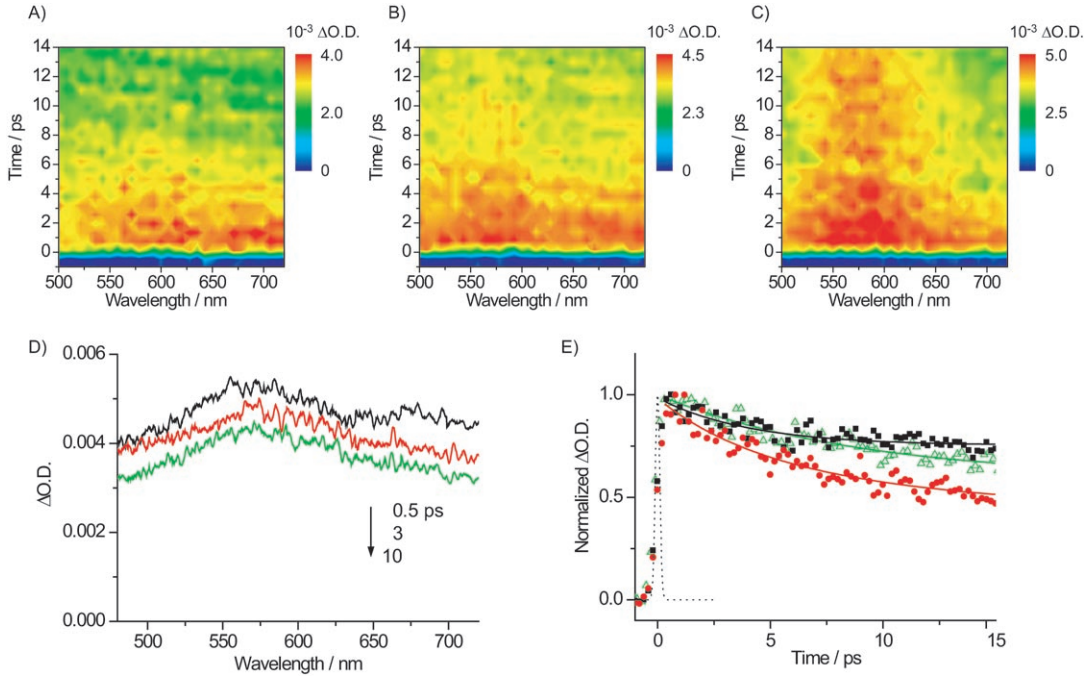


Figure 7. Time evolution of transient absorption spectra observed after the laser flash during the 330-nm laser photolysis of $TiO_2$ (A), $TiO_2$/CM-β-CD (B), and $TiO_2$/CM-β-CD/MTP (C) ([CM-β-CD] = 1 mM, [MTP] = 1 mM). D) The transient absorption spectra observed after the laser flash during the 330 nm laser photolysis of $TiO_2$/CM-β-CD/MTP ([CM-β-CD] = 1 mM, [MTP] = 1 mM). E) Normalized time traces observed at 575 (■) and 700 nm (●) after the laser flash during the 330 nm laser photolysis of $TiO_2$/CM-β-CD/MTP ([CM-β-CD] = 1 mM, [MTP] = 1 mM), and observed at 700 nm (△) after the laser flash during the 330-nm laser photolysis of $TiO_2$/CM-β-CD ([CM-β-CD] = 1 mM). The dotted line indicates a Gaussian function with an FWHM of 200 fs.

sites. There is a continuous energy-level dispersion for the localized levels, so that the carriers in the shallow trapping sites further relax into deep trapping sites by their migration. The trapping times of holes have been estimated to be less than 50 fs by Yang and Tamai[32] and $200 \pm 50$ fs by Furube et al.[35b] The difference in the trapping times could be explained in terms of the excitation-energy-dependent intraband relaxation of the hot holes. Considering the experimental results and the present excitation energy of 3.76 eV, the trapping times of the holes seemed to be less than our time resolution (200 fs).

Furube et al. have also reported that the hole relaxation from shallow sites to deep ones was occurring more than 100 ps after photoexcitation based on the spectral shift of the transient absorption.[35b] In fact, for the $TiO_2$ colloidal solution, we observed the spectral shift of the transient absorption within several tens of picoseconds owing to the hole relaxation from shallow sites to deep ones, and the recombination process with $e_{tr}^-$ of more than several hundreds of picoseconds (see Figure S3 in the Supporting Information). The decrease in the hole relaxation time by an order of magnitude might be due to the small particle size (4.5 nm) relative to the reported one (20 nm).

Therefore, the transit time of hot holes should be shorter than the decay constant of 4 ps observed for $TiO_2$/CM-β-CD/MTP,[46] suggesting that the interfacial hole transfer from $h_{VB}^+$ and shallow $h_{tr}^+$ to MTP included in CM-β-CD on $TiO_2$ occurs with the time constants of $<200$ fs and 4 ps, respectively. The observed fast interfacial hole transfer from $h_{VB}^+$ and shallow $h_{tr}^+$ to MTP would be due to the strong electronic interaction between MTP and $TiO_2$, because the diffusion rate primarily depends on the electronic coupling between the trapped states.[47] These trap sites span a wide range of energies, which can be modulated by chemical modification of the surface.[25,48]

**Decay processes of $S^{\bullet+}$**: It is worth clarifying the sequential reactions caused by $S^{\bullet+}$, because the efficiency of the photocatalytic reaction would be significantly dependent on the interfacial back electron transfer rate, which competes with many other reactions. The back electron transfer reaction between $e_{tr}^-$ and $S^{\bullet+}$ was influenced by numerous factors, for example, the relaxation time from the shallow to deep trap states, the oxidation potential of S, and the distance between the electron acceptor and the donor.

Figure 8 shows the time profiles observed at 545 (a) and 827 nm (b), which are mainly attributable to $MTPM^{\bullet+}$ and $e_{tr}^-$, respectively, after the laser flash during the 355 nm laser photolysis of the Ar-saturated $TiO_2$/CM-β-CD colloidal aqueous solution in the presence of MTPM (0.5 mM). No transient decay was observed for $e_{tr}^-$, suggesting that the decay process of $MTPM^{\bullet+}$ is not due to the charge recombination reaction with $e_{tr}^-$. Using the absorption coefficient values of $S^{\bullet+}$ ($\varepsilon^{\bullet+}$) (Table 1), the second-order rate constants ($k_d$) for the decay kinetics of $S^{\bullet+}$ were calculated to be $10^9$–$10^{10}\,M^{-1}s^{-1}$, as summarized in Table 5.

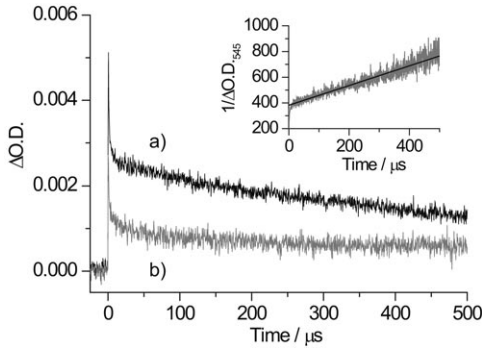


Figure 8. Time profiles observed at 545 (a) and 827 nm (b) after the laser flash during the 355 nm laser photolysis of the Ar-saturated $TiO_2$/CM-β-CD colloidal aqueous solution in the presence of MTPM (0.5 mM). Inset: second-order plots for the decay kinetics of $MTPM^{\bullet+}$ observed at 545 nm for the Ar-saturated $TiO_2$/CM-β-CD colloidal aqueous solution.

Table 5. Decay rate constants of $S^{\bullet+}$ in the microsecond time range.

| S | $k_d$ [$10^9$ M$^{-1}$ s$^{-1}$] | | |
|---|---|---|---|
| | water (pH 2)[a] | $TiO_2$ | $TiO_2$/CM-β-CD |
| MTP | 0.7±0.2 | 1.4±0.9 | 1.3±0.7 |
| MTT | 4.1±0.4 | 5.0±0.9 | 6.0±1.0 |
| MTPM | 4.1±0.4 | 4.6±1.0 | 4.0±1.0 |
| MTPA | 7.3±0.9 | 10±2 | 11±2 |

[a] Determined by pulse radiolysis.[20]

The determined $k_d$ values were similar to those determined in acidic water (pH 2). The similarity in behaviour observed for the decay of $S^{\bullet+}$ strongly suggests that $S^{\bullet+}$ is excluded from the CD host in the case of MTT or generated from the indirect one-electron oxidation reaction with $h_{tr}^+$ at the surface by a collisional process, and that the subsequent reaction occurs in the bulk solution, that is, outside the cavity in the microsecond time range. From the good second-order fits found for the decay process of $S^{\bullet+}$ in the presence of CM-β-CD, we can expect that the dissociation reaction takes place within several tens of microseconds. The complexation equilibrium between the CDs and a series of electroactive molecules, such as ferrocenes,[49] viologens,[50] and cobaltocenes,[51] has been investigated in detail and found to involve dissociation rate constants on the order of $10^4$ s$^{-1}$. Recently, Dimitrijevic et al. studied the photoinduced charge transfer between guest molecules and hybrid $TiO_2$/carboxyethyl-β-CD nanoparticles using low-temperature EPR and cyclic voltammetry.[6b] They used ferrocenemethanol ($K_{CD} = 2.1\times10^3$ M$^{-1}$) as the guest molecule and observed the formation of the ferrocenium cation, which is generated by an electron transfer from ferrocenemethanol to the $TiO_2$ nanoparticles, by UV irradiation. It was also mentioned that the dissociation of the charged ion from the hydrophobic cavity of carboxyethyl-β-CD into the bulk water leads to an efficient charge separation. Based on these experimental results and our recent work,[20] we can conclude that the generated $S^{\bullet+}$, especially $MTT^{\bullet+}$, inside CM-β-CD is excluded from the CD nanocavity attached on $TiO_2$ to give the free $S^{\bullet+}$ because of the hydrophobic nature of the cavity.

**Dimer radical cation formation**: Recently, we have clarified the formation and decay processes of the dimer radical cation of MTPM ($(MTPM)_2^{\bullet+}$) in the absence and presence of hydroxypropyl-β-CD by pulse radiolysis.[20] In order to clarify the dissociation and subsequent reactions of $S^{\bullet+}$, which is generated during the $TiO_2$ phototcatalytic reactions, we examined the influence of CM-β-CD on the formation process of $S_2^{\bullet+}$.

Figure 9 A shows the transient absorption spectra observed at 10 μs after the laser flash during the 355 nm laser photolysis of the Ar-saturated $TiO_2$ colloidal aqueous solution in the presence of CM-β-CD (0.5 mM) and MTPM (0.5, 5, and 10 mM).

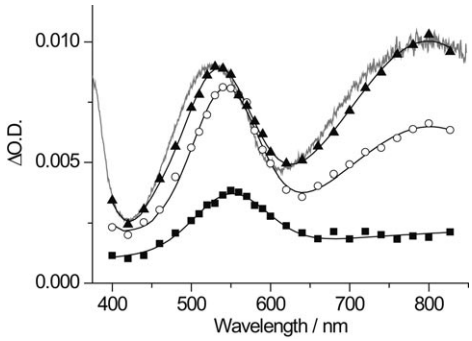


Figure 9. Transient absorption spectra observed at 10 μs after the laser flash during the 355 nm laser photolysis of the Ar-saturated $TiO_2$ colloidal aqueous solution in the presence of CM-β-CD (0.5 mM) and MTPM (0.5 (■), 5 (○), and 10 mM (▲). The gray line indicates the transient absorption spectrum obtained after an electron pulse during the pulse radiolysis of $N_2O$-saturated water (pH 2) in the presence of NaBr (100 mM) and MTPM (10 mM). The spectral intensity is normalized at 530 nm for comparison.

The absorption band around 550 nm observed at 10 μs after the laser pulse was blue-shifted by about 20 nm with the increasing MTPM concentration, while a new absorption band clearly appeared around 800 nm. Similar spectral changes were observed in the absence of CM-β-CD. The newly observed absorption bands at around 520 and 800 nm are assigned to the σ-type complex of the sulfur–sulfur three-electron bond and the π-type complex associated with two 4-(methylthio)phenyl groups, respectively.[18,52] The spectrum of $(MTPM)_2^{\bullet+}$, which is obtained by the pulse radiolysis technique, is also indicated for comparison (solid line).

The fact that the transient absorption spectra of $(MTPM)_2^{\bullet+}$, which are quite similar to that obtained from the pulse radiolysis measurements, were observed for $TiO_2$ and $TiO_2$/CM-β-CD suggests that $MTPM^{\bullet+}$ is generated from the indirect one-electron oxidation reaction with $h_{tr}^+$ and exists as a free molecule in solution, because only the free $MTPM^{\bullet+}$ can react with the free MTPM to give the free $(MTPM)_2^{\bullet+}$.[20]

  

**Overall reaction mechanisms**: We summarize the reaction schemes as follows. As a first step, $h_{VB}^+$ is generated by laser irradiation and then trapped at the surface of $TiO_2$ or the surface-bound CM-β-CD on $TiO_2$. Most of $h_{VB}^+$ and $h_{tr}^+$ recombine with $e_{CB}^-$ and $e_{tr}^-$ in the wide time range of femtoseconds to microseconds. In competition with the charge recombination processes, $h_{VB}^+$ and the shallow $h_{tr}^+$ are transferred to S adsorbed on the $TiO_2$ surface or included in CM-β-CD modified on the $TiO_2$ surface. The S having no hydroxy or carboxy groups, that is, MTT, included in CM-β-CD is oxidized by the CM-β-CD-mediated one-electron oxidation process with $h_{CD}^+$($CM^{\bullet+}$-β-CD) (Figure 10A).

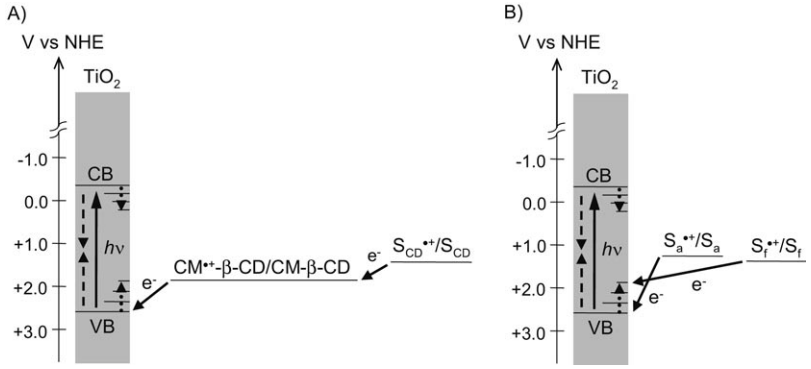


Figure 10. A) CM-β-CD-mediated one-electron oxidation process of $S_{CD}$ with $h_{CD}^+$. B) Direct and indirect one-electron oxidation processes of $S_a$ and $S_f$ with $h_{VB}^+$ and $h_{tr}^+$, respectively. Broken and dotted arrows represent the recombination and trapping processes of the photogenerated charge carriers, respectively. The $E_{ox}$ value of $S_a$ would be lower than that of $S_f$ owing to the adsorption on the $TiO_2$ surface.[53]

On the other hand, the S with hydroxy or carboxy groups included in the CM-β-CD can be directly adsorbed on the $TiO_2$ surface and oxidized by the direct one-electron oxidation process with $h_{VB}^+$ or the shallow $h_{tr}^+$ (Figure 10B). Free S is also oxidized by the indirect one-electron oxidation process with the deep $h_{tr}^+$ at the surface by a collision process (Figure 10B).

From the second-order fits found for the decay process of $S^{\bullet+}$, we can conclude that the dissociation process of $S^{\bullet+}$ from the CD nanocavity takes place during several microseconds, indicating that the dissociation rate constant should be higher than $10^5 \sim 10^6\ s^{-1}$. It was found that $S^{\bullet+}$ desorbed from CM-β-CD and/or generated from the indirect one-electron oxidation process with $h_{tr}^+$ can react with the free S to give $S_2^{\bullet+}$.

## Conclusion

We have successfully investigated the photocatalytic oxidation reactions of aromatic sulfides using CM-β-CD-modified $TiO_2$ nanoparticles ($TiO_2$/CM-β-CD) from nano- and femtosecond transient absorption measurements. The transient absorption spectra and time traces observed for the charge carriers and $S^{\bullet+}$ revealed that the one-electron oxidation reaction of S during the laser-flash photolysis of $TiO_2$/CM-β-CD is significantly enhanced when compared to the bare $TiO_2$. The kinetics of the decay and the dimerization processes between $S^{\bullet+}$s was discussed on the basis of the results obtained by the pulse radiolysis technique.

This work addresses several key issues in the fields of the $TiO_2$ photocatalysts and their hybrid nanomaterials with organic and inorganic compounds as follows: 1) the modification of the β-CDs with carboxyl groups on $TiO_2$ facilitates the charge-transfer interaction between organic compounds and $TiO_2$ nanoparticles, establishing efficient crosstalk between them; 2) a detailed examination of the formation dynamics of $S^{\bullet+}$ over a wide time scale from femto- to microseconds demonstrates that S is oxidized by $h_{VB}^+$, $h_{CD}^+$, and the shallow and deep $h_{tr}^+$s during the CM-β-CD-modified $TiO_2$ photocatalytic reactions; and 3) the release of $S^{\bullet+}$ from the CD nanocavity attached to the $TiO_2$ nanoparticles into the bulk solution is induced by the photocatalytic one-electron oxidation reaction, which might be applicable for novel drug delivery systems.

## Experimental Section

**Materials**: The β-CD (Aldrich) and carboxymethyl-β-CD (CM-β-CD) (Aldrich) were used without further purification. 4-(Methylthio)toluene (MTT) (Tokyo Kasei) was used without further purification. 4-(Methylthio)phenol (MTP) (Tokyo Kasei) and 4-(methylthio)phenyl methanol (MTPM) (Aldrich) were purified by vacuum sublimation before use. 4-(Methylthio)phenylacetic acid (MTPA) was recrystallized from ethanol.

The colloidal aqueous solutions of $TiO_2$ were prepared by the controlled hydrolysis of $TiCl_4$ at 0°C. In a typical preparation, fresh $TiCl_4$ (7.58 g, Wako) maintained at −10°C was slowly added dropwise over 1 h into of Milli-Q water (1 $dm^3$, 0°C) in a glass beaker with vigorous stirring. The $TiO_2$ colloidal solution (0.3 $dm^3$) was subsequently dialyzed at 4°C (Visking-tube presoaked for 1 week in approximately 2.5 $dm^3$ of Milli-Q water replaced several times per day) resulting in a pH of 2.0 for the colloidal solution ($[Cl^-] < 10^{-6}$ M). The concentration of the $TiO_2$ particles was $(2.9 \pm 1.0) \times 10^{-5}$ M. Transmission electron microscope (TEM) (JEOL, JEM-3000F, 200000×) and atomic force microscope (AFM) (Seiko Instruments Inc., SPA400-DFM, SI-DF20) images indicated that the mean particle size of the material was about 4.5 nm.

The aqueous solutions containing high concentrations of CDs were slowly added to the transparent $TiO_2$ colloidal aqueous solution and the mixtures were then thoroughly shaken and refrigerated until used. The number of β-CD and CM-β-CD bound to each $TiO_2$ nanoparticle in acidic water (pH 2) was estimated from the $^1H$ NMR measurements (Bruker, ARX 400). The concentrations of the surface-bound CDs were determined from the difference in the peak area of the sample solutions, which were obtained by dialyzing water and the $TiO_2$ colloidal solution

  

against CD solutions until an adsorption equilibrium was reached. The spectra were normalized using a capillary of acetone as the external standard.

**Steady-state UV/Vis absorption measurements**: The steady-state UV/Vis absorption spectra were measured by an UV-VIS-NIR spectrophotometer (Shimadzu, UV-3100) at room temperature.

**Nanosecond transient absorption measurements**: The nanosecond laser-flash photolysis experiments were performed by using the third harmonic generation (355 nm, 5 ns FWHM) from a Q-switched $Nd^{3+}$:YAG laser (Continuum, Surelite II-10) for the excitation operated with temporal control by a delay generator (Stanford Research Systems, DG535). The analyzing light from a 450-W Xe-arc lamp (Ushio, UXL-451–0) was collected by a focusing lens and directed through a grating monochromator (Nikon, G250) to a silicon avalanche photodiode detector (Hamamatsu Photonics, S5343). The analyzing lamp, sample, monochromator, and a silicon avalanche photodiode detector all lie on the same axis with the excitation beam incident at 90° to the axis. The transient signals were recorded with a digitizer (Tektronix, TDS 580D). To avoid stray light and pyrolysis of the sample by the probe light, suitable filters were employed. The irradiation energy was measured using a power meter. All measurements were carried out at room temperature.

**Femtosecond transient absorption measurements**: The femtosecond transient absorption spectra were measured by the pump and probe method using a regeneratively amplified titanium sapphire laser (Spectra Physics, Spitfire Pro F, 1 kHz) pumped by a Nd:YLF laser (Spectra Physics, Empower 15). The seed pulse was generated by a titanium sapphire laser (Spectra-Physics, Tsunami 3941 M1BB, 80 fs FWHM) pumped with a diode-pumped solid state laser (Spectra-Physics, Millennia VIIIs). The fourth harmonic generation (330 nm, 5 μJ $pulse^{-1}$) of the optical parametric amplifier (Spectra Physics, OPA-800CF-1) or a second harmonic generation of the fundamental (400 nm, 10 μJ $pulse^{-1}$) were used as the excitation pulse. The excitation light was depolarized. A white light continuum pulse, which was generated by focusing the residual of the fundamental light on the flowing water cell after the computer-controlled optical delay, was divided into two parts and used as the probe and the reference lights, of which the latter was used to compensate the laser fluctuation. Both the probe and reference lights were directed to the rotating sample cell with a 1.0-mm optical path and detected by the CCD detector equipped with the polychromator (Solar, MS3504). The pump pulse was chopped by the mechanical chopper synchronized to one half of the laser repetition rate, resulting in a pair of spectra with and without the pump, from which the absorption change induced by the pump pulse was estimated. All measurements were carried out at room temperature.

**Pulse radiolysis measurements**: The Pulse radiolysis experiments were performed using an electron pulse (28 MeV, 8 ns, 0.87 kGy per pulse) from a linear accelerator at Osaka University. All experiments were performed with aqueous acidic solutions (pH 2) that had been saturated with purified $N_2O$ gas for a minimum of 20 min by using a capillary technique. The kinetic measurements were performed using a nanosecond photoreaction analyzer system (Unisoku, TSP-1000).[20]

## Acknowledgements

The authors wish to thank the people in the Radiation Laboratory, The Institute of Scientific and Industrial Research, Osaka University, for running the pulse radiolysis. The authors are grateful to Dr. Yoshio Takai for $^1$H NMR measurements. This work has been partly supported by a Grant-in-Aid for Scientific Research (Project 17105005, Priority Area (417), 21 st Century COE Research, and others) from the Ministry of Education, Culture, Sports, Science and Technology (MEXT) of Japanese Government.

[1] For example: a) D. M. Adams, L. Brus, C. E. D. Chidsey, S. Creager, C. Creutz, C. R. Kagan, P. V. Kamat, M. Lieberman, S. Lindsay, R. A. Marcus, R. M. Metzger, M. E. Michel-Beyerle, J. R. Miller, M. D. Newton, D. R. Rolison, O. Sankey, K. S. Schanze, J. Yardley, X. J. Zhu, *J. Phys. Chem. B* **2003**, *107*, 6668–6697; b) E. Katz, I. Willner, *Angew. Chem.* **2004**, *116*, 6166–6235; *Angew. Chem. Int. Ed.* **2004**, *43*, 6042–6108; c) N. L. Rosi, C. A. Mirkin, *Chem. Rev.* **2005**, *105*, 1547–1562; d) T. Paunesku, T. Rajh, G. Wiederrecht, J. Maser, S. Vogt, N. Stojićević, M. Protić, B. Lai, J. Oryhon, M. Thurnauer, G. Woloschak, *Nat. Mater.* **2003**, *2*, 343–346; e) N. M. Dimitrijevic, Z. V. Saponjic, B. M. Rabatic, T. Rajh, *J. Am. Chem. Soc.* **2005**, *127*, 1344–1345.

[2] For example: a) J. Szejtli, *Chem. Rev.* **1998**, *98*, 1743–1753; b) *Comprehensive Supermolecular Chemistry, Vol. 3* (Eds.: J. Szejtli, T. Osa), Pergamon, New York, **1996**; c) M. E. Davis, M. E. Brewster, *Nature Rev. Drug Deliv.* **2004**, *3*, 1023–1035; d) A. Harada, *Acc. Chem. Res.* **2001**, *34*, 456–464.

[3] M. Yoon, D. Anandan, *Catal. Commun.* **2004**, *5*, 271–275.

[4] P. Lu, F. Wu, W. Deng, *Appl. Catal. B* **2004**, *53*, 87–93.

[5] a) I. Willner, Y. Eichen, *J. Am. Chem. Soc.* **1987**, *109*, 6862–6863; b) I. Willner, Y. Eichen, A. J. Frank, *J. Am. Chem. Soc.* **1989**, *111*, 1884–1886; c) I. Willner, Y. Eichen, B. Willner, *Res. Chem. Intermed.* **1994**, *20*, 681–700.

[6] a) N. M. Dimitrijevic, Z. V. Saponjic, D. M. Bartels, M. C. Thurnauer, D. M. Tiede, T. Rajh, *J. Phys. Chem. B* **2003**, *107*, 7368–7375; b) N. M. Dimitrijevic, T. Rajh, Z. V. Saponjic, L. de la Garza, D. M. Tiede, *J. Phys. Chem. B* **2004**, *108*, 9105–9110.

[7] J. Feng, A. Miedaner, P. Ahrenkiel, M. E. Himmel, C. Curtis, D. Ginley, *J. Am. Chem. Soc.* **2005**, *127*, 14968–14969.

[8] S. A. Haque, J. S. Park, M. Srinivasarao, J. R. Durrant, *Adv. Mater.* **2004**, *16*, 1177–1181.

[9] a) K. A. Connors, *Chem. Rev.* **1997**, *97*, 1325–1357; b) M. V. Rekharsky, Y. Inoue, *Chem. Rev.* **1998**, *98*, 1875–1917.

[10] L. Liu, Q. -X. Guo, *J. Phys. Chem. B* **1999**, *103*, 3461–3467.

[11] C. Chatgilialoglu, M. P. Bertrand, C. Ferreri, "Sulfur-Centered Radicals in Organic Synthesis" in *S-Centered Radicals* (Ed.: Z. B. Alfassi), Wiley, Chichester, UK, **1999**, pp. 311–354.

[12] T. Tobien, W. J. Cooper, M. G. Nickelsen, E. Pernas, K. E. O'Shea, K.-D. Asmus, *Environ. Sci. Technol.* **2000**, *34*, 1286–1291.

[13] S. Ozaki, P. R. Ortiz de Montelano, *J. Am. Chem. Soc.* **1995**, *117*, 7056–7064.

[14] P. Wardman, "Thiyl Radicals in Biology: Their Role as a "Molecular Switch" Central to Cellular Oxidative Stress" in *S-centered Radicals* (Ed.: Z. B. Alfassi), Wiley, Chichester, UK, **1999**, pp. 289–309.

[15] M. Ioele, S. Steenken, E. Baciocchi, *J. Phys. Chem. B* **1997**, *101*, 2979–2987.

[16] H. Mohan, J. P. Mittal, *Bull. Chem. Soc. Jpn.* **2001**, *74*, 1649–1659.

[17] H. Mohan, J. P. Mittal, *J. Phys. Chem. A* **2002**, *106*, 6574–6580.

[18] H. Yokoi, A. Hatta, K. Ishiguro, Y. Sawaki, *J. Am. Chem. Soc.* **1998**, *120*, 12728–12733.

[19] a) T. Tachikawa, S. Tojo, M. Fujitsuka, T. Majima, *Chem. Phys. Lett.* **2003**, *382*, 618–625; b) S. Tojo, T. Tachikawa, M. Fujitsuka, T. Majima, *Chem. Phys. Lett.* **2004**, *384*, 312–316; c) S. Tojo, T. Tachikawa, M. Fujitsuka, T. Majima, *Phys. Chem. Chem. Phys.* **2004**, *6*, 960–964; d) T. Tachikawa, S. Tojo, M. Fujitsuka, T. Majima, *J. Phys. Chem. B* **2004**, *108*, 5859–5866; e) T. Tachikawa, A. Yoshida, S. Tojo, A. Sugimoto, M. Fujitsuka, T. Majima, *Chem. Eur. J.* **2004**, *10*, 5345–5353.

[20] T. Tachikawa, S. Tojo, M. Fujitsuka, T. Majima, *J. Phys. Chem. B* **2005**, *109*, 17460–17466.

[21] J. Reuben, C. T. Rao, J. Pitha, *Carbohydr. Res.* **1994**, *258*, 281–285.

[22] a) For 4.5 nm particles, there are about 400 surface Ti atoms per particle,[6b] thus with the ratio of CD to particles as low as 6:1, there is more than 95% free unmodified surface Ti sites capable of trapping electrons. The $pK_a$ of CM-β-CD is assumed to be near 3.75 based on the previously reported value of a closely related carboxylated CD (carboxymethylethyl-β-CD);[22b] b) K. Uekama, Y. Horiuchi, T. Irie, F. Hirayama, *Carbohydr. Res.* **1989**, *192*, 323–330.

[23] S. Tunesi, M. A. Anderson, *Langmuir* **1992**, *8*, 487–495.

[24] a) T. Rajh, L. X. Chen, K. Lukas, T. Liu, M. C. Thurnauer, D. M. Tiede, *J. Phys. Chem. B* **2002**, *106*, 10543–10552; b) P. C. Redfern,

  

P. Zapol, L. A. Curtiss, T. Rajh, M. C. Thurnauer, *J. Phys. Chem. B* **2003**, *107*, 11419–11427.
[25] Y. S. Seo, C. Lee, K. H. Lee, K. B. Yoon, *Angew. Chem.* **2005**, *117*, 932–935; *Angew. Chem. Int. Ed.* **2005**, *44*, 910–913; .
[26] T. Tachikawa, S. Tojo, M. Fujitsuka, T. Majima, *Langmuir* **2004**, *20*, 2753–2759.
[27] A. P. Scott, L. Radom, *J. Phys. Chem.* **1996**, *100*, 16502–16513.
[28] Gaussian 98 (Revision A.7), M. J. Frisch, G. W. Trucks, H. B. Schlegel, G. E. Scuseria, M. A. Robb, J. R. Cheeseman, V. G. Zakrzewski, J. A. Montgomery, R. E. Stratmann, J. C. Burant, S. Dapprich, J. M. Millam, A. D. Daniels, K. N. Kudin, M. C. Strain, O. Farkas, J. Tomasi, V. Barone, M. Cossi, R. Cammi, B. Mennucci, C. Pomelli, C. Adamo, S. Clifford, J. Ochterski, G. A. Petersson, P. Y. Ayala, Q. Cui, K. Morokuma, D. K. Malick, A. D. Rabuck, K. Raghavachari, J. B. Foresman, J. Cioslowski, J. V. Ortiz, A. G. Baboul, B. B. Stefanov, G. Liu, A. Liashenko, P. Piskorz, I. Komaromi, R. Gomperts, R. L. Martin, D. J. Fox, T. Keith, M. A. Al-Laham, C. Y. Peng, A. Nanayakkara, C. Gonzalez, M. Challacombe, P. M. W. Gill, B. G. Johnson, W. Chen, M. W. Wong, J. L. Andres, M. Head-Gordon, E. S. Replogle, J. A. Pople, Gaussian, Inc., Pittsburgh, PA, **1998**.
[29] a) G. Rothenberger, J. Moser, M. Grätzel, N. Serpone, D. K. Sharma, *J. Am. Chem. Soc.* **1985**, *107*, 8054–8059; b) N. Serpone, D. Lawless, R. Khairutdinov, E. Pelizzetti, *J. Phys. Chem.* **1995**, *99*, 16655–16661.
[30] a) D. Bahnemann, A. Henglein, J. Lilie, L. Spanhel, *J. Phys. Chem.* **1984**, *88*, 709–711; b) D. W. Bahnemann, M. Hilgendorff, R. Memming, *J. Phys. Chem. B* **1997**, *101*, 4265–4275.
[31] a) D. P. Colombo, Jr., R. M. Bowman, *J. Phys. Chem.* **1995**, *99*, 11752–11756; b) D. P. Colombo, Jr., R. M. Bowman, *J. Phys. Chem.* **1996**, *100*, 18445–18449.
[32] X. Yang, N. Tamai, *Phys. Chem. Chem. Phys.* **2001**, *3*, 3393–3398.
[33] K. Iwata, T. Takaya, H. Hamaguchi, A. Yamakata, T. Ishibashi, H. Onishi, H. Kuroda, *J. Phys. Chem. B* **2004**, *108*, 20233–20239.
[34] a) A. Furube, T. Asahi, H. Masuhara, H. Yamashita, M. Anpo, *J. Phys. Chem. B* **1999**, *103*, 3120–3127; b) A. Furube, T. Asahi, H. Masuhara, H. Yamashita, M. Anpo, *Res. Chem. Intermed.* **2001**, *27*, 177–187.
[35] a) T. Yoshihara, R. Katoh, A. Furube, Y. Tamaki, M. Murai, K. Hara, S. Murata, H. Arakawa, M. Tachiya, *J. Phys. Chem. B* **2004**, *108*, 3817–3823; b) Y. Tamaki, A. Furube, R. Katoh, M. Murai, K. Hara, H. Arakawa, M. Tachiya, *C. R. Chim.* **2006**, *9*, 268–274; c) Y. Tamaki, A. Furube, M. Murai, K. Hara, R. Katoh, M. Tachiya, *J. Am. Chem. Soc.* **2006**, *128*, 416–417.
[36] a) I. A. Shkrob, M. C. Sauer, Jr., *J. Phys. Chem. B* **2004**, *108*, 12497–12511; b) I. A. Shkrob, M. C. Sauer, Jr., D. Gosztola, *J. Phys. Chem. B* **2004**, *108*, 12512–12517.
[37] a) To date, three distinguishable $h_{tr}^+$ have been reported by several groups. For example, Katoh and co-workers reported that the absorption spectrum of $h_{tr}^+$ has peaks at 520 and ~1200 nm from the nanosecond transient absorption measurements.[35a] They mentioned that the peak position reflects the trap depth of $h_{tr}^+$, that is, the $h_{tr}^+$ with the peak at 520 nm was trapped deeper than that with the peak at 1200 nm, although the origin of the absorption peaks is unclear. Shkrob et al. also suggested that $h_{tr}^+$ with the peak at 520 nm could be assigned to the TiO˙Ti (an undercoordinated titanium atom) at the surface, and not to a surface-bound ·OH radical.[36] On the other hand, some groups reported the surface-bound ˙OH radical, which has a peak at about 350 nm, using a pulse radiolysis technique;[19b, 37b] b) D. Lawless, N. Serpone, D. Meisel, *J. Phys. Chem.* **1991**, *95*, 5166–5170.
[38] a) Assuming that the same number of charge carriers was generated during the 355 nm laser photolysis of the $TiO_2$ colloidal aqueous solution, $\varepsilon$ for $h_{tr}^+$ was estimated from the $\varepsilon$ value of $700\,M^{-1}\,cm^{-1}$ at 800 nm for $e^-$.[38b,c] The spectral shape was identical within the experimental error in the present time period (<30 μs), suggesting that the charge recombination between $e^-$ and $h^+$ occurred without quenching by some impurities and trapping into other sites; b) A. Safrany, R. Gao, J. Rabani, *J. Phys. Chem. B* **2000**, *104*, 5848–5853; c) T. Tachikawa, S. Tojo, M. Fujitsuka, T. Majima, *Langmuir* **2004**, *20*, 9441–9444.
[39] T. Tachikawa, S. Tojo, M. Fujitsuka, T. Majima, *Chem. Eur. J.* in press.
[40] a) Several researchers have reported that ·OH radicals diffuse away from the surface of the $TiO_2$ particles and react with scavengers in the bulk solution.[40b] In general, the reaction of ˙OH radical with thioanisoles results in the formation of radical cations and OH adducts. However, we could not confirm the formation of the OH adducts because they have absorption in the UV region. For example, the transient species generated by the addition of ˙OH radicals to the benzene ring and the sulfur center of MTPM show the transient absorption bands at 320 and 360 nm, respectively;[16] b) M. R. Hoffmann, S. T. Martin, W. Choi, D. W. Bahnemann, *Chem. Rev.* **1995**, *95*, 69–96.
[41] O. I. Micic, T. Rajh, M. V. Comor in *Electrochemistry in Colloids and Dispersions* (Eds.: R. A. Mackey, J. Texter), VCH, New York, **1992**, p. 457.
[42] a) P. V. Kamat, M. A. Fox, *Chem. Phys. Lett.* **1983**, *102*, 379–384; b) P. V. Kamat, K. R. Gopidas, D. Weir, *Chem. Phys. Lett.* **1988**, *149*, 491–496.
[43] K. Kalyanasundaram, N. Vlachopoulos, V. Krishnan, A. Monnier, M. Grätzel, *J. Phys. Chem.* **1987**, *91*, 2342–2347.
[44] Y.-X. Weng, Y.-Q. Wang, J. B. Asbury, H. N. Ghosh, T. Lian, *J. Phys. Chem. B* **2000**, *104*, 93–104.
[45] a) J. N. Clifford, G. Yahioglu, L. R. Milgrom, J. R. Durrant, *Chem. Commun.* **2002**, 1260–1261; b) E. Topoglidis, C. J. Campbell, E. Palomares, J. R. Durrant, *Chem. Commun.* **2002**, 1518–1519; c) J. N. Clifford, E. Palomares, M. K. Nazeeruddin, M. Grätzel, J. Nelson, X. Li, N. J. Long, J. R. Durrant, *J. Am. Chem. Soc.* **2004**, *126*, 5225–5233.
[46] a) The average transit time ($\tau_{av}$) for a hole from the interior to the surface of particle can be calculated by $\tau_{av} = R^2/\pi^2 D_h$, where $R$ is the radius of the particles and $D_h$ is the diffusion coefficient of the hole at room temperature ($D_h = 4\times10^{-5}\,m^2\,s^{-1}$).[46b] Thus, $\tau_{av}$ is calculated to be about 50 fs, which might be on the same order of magnitude as the hole trapping time; b) B. Enright, D. Fitzmaurice, *J. Phys. Chem.* **1996**, *100*, 1027–1035.
[47] M. O'Neil, J. Marohn, G. McLendon, *Chem. Phys. Lett.* **1990**, *168*, 208–210.
[48] T. Dannhauser, M. O'Neil, K. Johanssen, D. Whitten, G. McLendon, *J. Phys. Chem.* **1986**, *90*, 6074–6076.
[49] T. Matsue, D. H. Evans, T. Osa, N. Kobayashi, *J. Am. Chem. Soc.* **1985**, *107*, 3411–3417.
[50] Y. Wang, S. Mendoza, A. E. Kaifer, *Inorg. Chem.* **1998**, *37*, 317–320.
[51] A. E. Kaifer, *Acc. Chem. Res.* **1999**, *32*, 62–71.
[52] In the case of MTP, the transient absorption spectra attributed to $(MTP)_2^{\bullet+}$ were not observed in the absence and presence of CM-β-CD, although $MTP^{\bullet+}$ was clearly observed. MTP has a strong electron donating −OH group, and hence the delocalization of the positive charge over the aromatic rings is more effective than that in MTPM. Therefore, the formation of $S_2^{\bullet+}$ is unfavourable and could not be clearly observed for MTP. Unfortunately, we cannot observe the transient absorption spectra of $S_2^{\bullet+}$ for MTT and MTPA because of their poor solubility in acidic water.
[53] E. Galoppini, W. Guo, W. Zhang, P. G. Hoertz, P. Qu, G. J. Meyer, *J. Am. Chem. Soc.* **2002**, *124*, 7801–7811.

Received: January 22, 2006
Published online: July 6, 2006

  